Available online at www.sciencedirect.com
SCIENCE DIRECT
Journal of Catalysis 241 (2006) 115–122
JOURNAL OF CATALYSIS
www.elsevier.com/locate/jcat

Theoretical study of dehydrogenation and isomerisation reactions of propylene on Pt(111)

Ana Valcárcel [a,*], Josep M. Ricart [a,*], Anna Clotet [a], Francesc Illas [b], Alexis Markovits [c], Christian Minot [c]

[a] *Departament de Química Física i Inorgànica, Universitat Rovira i Virgili, C/Marcel·lí Domingo s/n, E-43007 Tarragona, Spain*
[b] *Departament de Química Física i Centre Especial de Recerca en Química Teòrica, Universitat de Barcelona i Parc Científic de Barcelona, C/Martí i Franquès 1, E-08028 Barcelona, Spain*
[c] *Laboratoire de Chimie Théorique, UMR-CNRS 7616, Université Pierre et Marie Curie, 4 place Jussieu, 75252 Paris cédex 05, France*

Received 1 December 2005; revised 3 April 2006; accepted 4 April 2006

Available online 30 May 2006

Abstract

We have investigated the thermodynamics of the dehydrogenation of propylene to propylidyne on Pt(111) for a 0.25 ML coverage. We have also determined the adsorption energies and most favourable adsorption sites for propylene, propylidyne, and all of the C_3H_x ($x = 3$–7) intermediates (1-propyl, 2-propyl, propylidene, 1-propenyl, 2-propenyl, propenylidene, and propynyl). All surface species are more stable than gas-phase propylene. Propylidyne is found to be the most stable species at the surface, in agreement with previous experiments. All surface moieties adsorb on sites where the metal atoms replace the missing hydrogen, thereby preserving a sp^3 hybridisation of the C atoms of the adsorbed hydrocarbon. We used the adsorption energies to compute the overall reaction energies for a total of 18 elementary C–H bond activation and isomerisation reactions that are likely to be involved in the dehydrogenation of propylene. The combination of energy and vibrational frequency calculations allowed us to propose some species as possible intermediates of the decomposition process—propylidene and 1-propenyl.

Keywords: Propylene; Propylidyne; Platinum; Pt(111); Dehydrogenation; Chemisorption; Catalysis; DFT

1. Introduction

Fundamental studies of alkene chemistry over catalytically active transition metal surfaces play a key role in guiding subsequent efforts to understand and improve diverse catalytic processes ranking from pollution control to fine chemical synthesis. Consequently, the chemisorption of olefins has been extensively investigated with a view toward determining adsorption geometries and the nature and stability of reaction intermediates and products [1]. A first approach to the study of the hydrocarbon surface chemistry is achieved by single-crystal model surfaces [2–5], thus avoiding the complexities of the actual catalysts. The interaction of ethylene ($CH_2{=}CH_2$) with Pt(111) has been extensively used as a model system to understand alkene hydrogenation–dehydrogenation processes. At low temperatures, ethylene adsorbs on the Pt(111) surface in a di-σ mode, forming a (2×2) pattern. On heating to above 300 K, it transforms into a new, more stable species, ethylidyne [6–8]. A (2×2) structure is revealed after exposure to the electron beam of a LEED gun. This molecule is stable at the surface roughly between 300 and 420 K. The ethylene-to-ethylidyne transition represents a whole class of reactions, namely the dehydrogenation of alkenes to alkylidynes. This reaction is believed to be involved in catalytic hydrogenation and dehydrogenation processes. To obtain ethylidyne, one H atom must migrate from one C atom to another, and a second H atom must be removed from the molecule. Then it is reasonable to assume that the mechanism comprises at least two steps and involves the formation of one or more intermediates.

* Corresponding authors.
E-mail addresses: anaval@urv.net (A. Valcárcel), josep.ricart@urv.net (J.M. Ricart).

0021-9517/$ – see front matter
doi:10.1016/j.jcat.2006.04.022

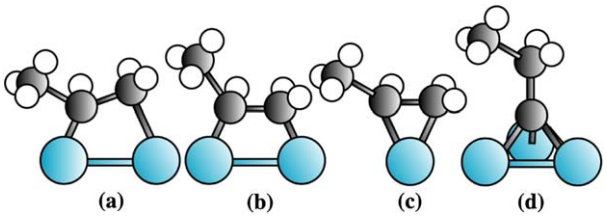

Scheme 1. Surface structures for the adsorption of propylene on Pt(111): propylene di-σ V-shape (a), propylene di-σ (b), propylene π (c), propylidyne (d). White, H, grey, C and light blue, Pt atoms. (For interpretation of the references to colour in this scheme legend, the reader is referred to the web version of this article.)

The details of this surface process have been subject of intense debate. Several simple mechanisms have been proposed with ethyl ($CH_3CH_2^{\bullet}$), vinyl ($CH_2CH^{\bullet}$), ethylidene ($CH_3CH^{\bullet}$), and/or vinylidene ($CH_2C^{\bullet}$) intermediates [9–15].

The attempt to extend the preceding conclusions to other olefins has been unsuccessful, because much less information is available for heavier alkenes. It has been also proposed that heavier alkenes decompose via the corresponding alkylidyne intermediates. After ethylene, propylene ($CH_3CH{=}CH_2$) is the most important raw material used in the production of organic chemicals. Early in 1982, Salmerón and Somorjai showed that propylene adsorbs easily on Pt(111) and remains stable with no chemical decomposition up to around 280 K [16]. Using thermal desorption spectroscopy (TDS), these authors estimated an adsorption energy of -51 kJ mol^{-1} at low coverage. Koestner et al. [8], using low-energy electron diffraction (LEED), proposed that propylene binds to two surface Pt atoms through its unsaturated C=C unit (di-σ-bond) and forms a disordered monolayer. Their results are in agreement with more recent experimental works [17,18] and with the results derived from qualitative molecular orbital calculations [19]. In addition, Koel et al. also investigated the adsorption and decomposition of propylene on Pt(111) [20] and determined an adsorption energy of ~ -70 kJ mol^{-1}. However, this rather simple picture of the interaction of propylene with Pt(111) contrasts with the complexity that emerges from the complete reflection–absorption (RAIRS) studies of Zaera and Chrysostomou [21]. Those authors proposed that at least four species derive from adsorbed propylene, depending on coverage and temperature. For the sake of clarity, we created a schematic representation of these surface structures (Scheme 1). At temperatures below 230 K, this molecule adsorbs undissociated on Pt(111) analogously to ethylene [22]. Below half-saturation, propylene binds preferentially to the metal surface in a di-σ fashion through its central C bond (V-shape; Scheme 1a). As the coverage increases up to saturation, the molecule rearranges, the C=C bond becomes more parallel to the surface, and the methyl group tilts away from the surface toward a more vertical orientation (Scheme 1b). Comparing infrared data from propylene ligands in osmium organometallic complexes with electron energy loss spectrometry (EELS) and RAIRS data for propylene on Pt(111) and on Ni(111) [23] corroborates the di-σ adsorption mode with significant rehybridisation of the C atoms toward sp^3. However, this comparison does not provide further information on the structure of the adsorbed molecule. Above saturation coverage, a second layer of weakly adsorbed molecules grows (π-bonded; Scheme 1c), and a clear transformation between about 230 and 270 K has been observed [23]. Actually, the 275 K RAIRS spectrum is consistent with the formation of propylidyne ($CH_3CH_2C^{\bullet}$; Scheme 1d), an alkylidyne moiety. The formation of an intermediate during the transformation from propylene to propylidyne seems evident according to the new feature at 2890 cm^{-1} observed in the 256 and 268 K RAIRS spectra [23]. This signal cannot be associated with propylene or with propylidyne, but may be related to 2-propyl ($CH_3(CH_3)CH^{\bullet}$) or propylidene ($CH_3CH_2CH^{\bullet}$) species. Koestner et al. [8] also detected formation of the propylidyne species and found that the LEED-IV spectra of ethylene and propylene are roughly identical between 280 and 400 K. This seems to indicate that the room temperature propylene has a structure similar to that of room temperature ethylene. The data are consistent with the presence of an alkylidyne species. In contrast to the nonspontaneous ordering of ethylidyne, propylidyne forms spontaneously a 2×2 pattern due to steric considerations.

Table 1
Surface species (C_3H_x, $x = 3$–7) listed in decreasing value of x

Name	Molecular formula	Structure
1-Propyl	C_3H_7	$CH_3CH_2CH_2^{\bullet}$
2-Propyl	C_3H_7	$CH_3(CH_3)CH^{\bullet}$
Propylene	C_3H_6	$CH_3CH{=}CH_2$
Propylidene	C_3H_6	$CH_3CH_2CH^{\bullet}$
Propylidyne	C_3H_5	$CH_3CH_2C^{\bullet}$
1-Propenyl	C_3H_5	$CH_3CH{=}CH^{\bullet}$
2-Propenyl	C_3H_5	$CH_3C^{\bullet}{=}CH_2$
Propenylidene	C_3H_4	$CH_3CH{=}C^{\bullet}$
Propyne	C_3H_4	$CH_3C{\equiv}CH$
Propynyl	C_3H_3	$CH_3C{\equiv}C^{\bullet}$

Clearly, deriving accurate descriptions of the structures of propylene, propylidyne, and the possible reaction intermediates (see Table 1) is a necessary step in understanding the subsequent surface processes. Toward this end, we used periodic density functional theory (DFT) calculations to determine the geometry, adsorption site preference, and adsorption energy for these species. We also carried out an analysis of vibrational spectra. Here we focus our discussion on the comparison with available experimental data.

2. Computational details

We obtained the geometries and energies of the relevant species adsorbed on Pt(111) from DFT calculations on a two-dimensional four-layer slab model of Pt(111) generated in a three-dimensional periodic supercell by introducing a vacuum width in the direction perpendicular to the surface (~12 Å). We carried out the DFT calculations using the generalized gradient approximation (GGA) exchange-correlation potential of Perdew and Wang [24]. The Kohn–Sham equations of the DFT were solved in a plane wave basis set, with the effect of core electrons in the one-electron functions taken into account through the projector-augmented wave (PAW) method [25]. Tight convergence of the plane-wave expansion was achieved

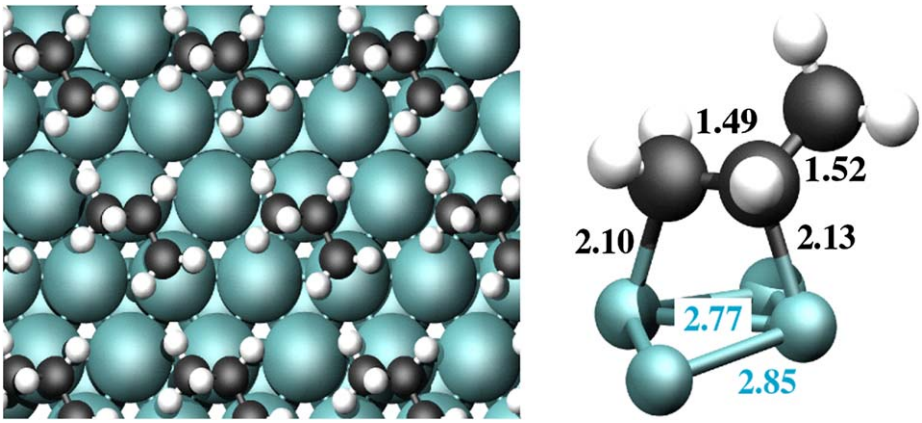

Fig. 1. 2 × 2 unit cell of propylene on Pt(111). Only the atoms directly below the hydrocarbon moiety are shown. All distances are in Å.

with a cutoff of 400 eV. For our purposes, we considered a 2×2 unit cell associated with a molecular coverage of 0.25 ML. This corresponds to the experimentally determined structure for propylidyne on Pt(111) [8]. The 2D Brillouin integrations were performed on a $7 \times 7 \times 1$ Monkhorst–Pack grid.

We obtained the geometry of the different adsorbed species by total energy minimisation with respect to the degrees of freedom of the adsorbates and of the two uppermost atomic metal layers; the rest of metal planes were kept fixed at the calculated bulk geometry with a Pt–Pt interatomic distance of 2.82 Å. The adsorption energies (E_{ads}) were obtained using

$$E_{\text{ads}} = (E_{\text{C}_3\text{H}_x/\text{surface}} - E_{\text{surface}} - E_{\text{C}_3\text{H}_{6(\text{g})}}) - (x-6)(E_{\text{H/surface}} - E_{\text{surface}}), \quad (1)$$

where a negative value indicates an exothermic chemisorption process. Eq. (1) allowed us to obtain adsorption energies of the different surface intermediates, which can be directly compared with the propylene adsorption energy.

We computed the vibrational frequencies and the corresponding normal modes within the harmonic approach, neglecting the coupling between molecular vibrations and surface phonons. This allowed us to rely on the block of the Hessian matrix involving adsorbate atomic displacements only. The harmonic molecular frequencies and the associated normal modes were directly obtained by diagonalisation of the corresponding block of the mass-pondered Hessian matrix. The energy second derivatives were obtained from numerical differences of the analytical gradients. We calculated the IR intensities through the following equation:

$$I^k = \left(\frac{\mathrm{d}\mu_z}{\mathrm{d}Q_k}\right)^2 = \left(\sum_{i=1}^{3N} \frac{P_{ki}}{\sqrt{m_i}} \frac{\mathrm{d}\mu_z}{\mathrm{d}\Delta r_i}\right)^2, \quad (2)$$

where μ_z is the z-component of the dipole moment and $P_{ki}/\sqrt{m_i}$ is the mass weighted coordinate matrix of the normal mode. We performed the numerical calculation of the first derivative of the dipole moment in the Cartesian coordinate system (Δr_i). We carried out all calculations using the Vienna Ab Initio Simulation Program (VASP) [26–28].

3. Results

3.1. Adsorption of propylene, propylidyne, and C_3H_x ($x = 3$–7) intermediates on Pt(111)

In a previous paper [29], we showed that propylene adsorbs preferentially on Pt(111) in a di-σ mode [$\eta^1\eta^1(\text{C}^1,\text{C}^2)$-adsorption mode; Fig. 1]. Our calculations were in good agreement with the results of Zaera and Chrysostomou [21] (see Scheme 1b). In the earlier work, we did not consider the effect of surface relaxation and used US-PP pseudopotentials. In this paper we reexamine the propylene–surface interaction, taking surface relaxation explicitly into account and using PAW. As expected, the changes on the substrate were rather small; the relaxation of the surface metal atoms involved mainly a small outward displacement of the Pt atoms directly interacting with the C atoms. This produced a small corrugation of the surface (<4%) with the simultaneous change in the Pt–Pt bond distances (<0.16 Å). However, the adsorption energy changed significantly, from -39 kJ mol^{-1} [29] (nonrelaxed surface, US-PP) and -66 kJ mol^{-1} (nonrelaxed surface, PAW) to -87 kJ mol^{-1} (relaxed surface, PAW). The computed adsorption energy was noticeably larger than the value estimated by TDS experiments: -50 kJ mol^{-1} [16] and -70 kJ mol^{-1} [20]. This is not surprising, because the tendency of PW91 to overestimate adsorption energies is well established [30]. Moreover, it is difficult to compare the calculated value with the experimental adsorption energy from TDS curves, because propylene decomposition may occur before desorption takes place at around 270–280 K [21]. Zaera and Chrysostomou [21] proposed that below saturation coverage, the hydrogen atom released in the dehydrogenation reaction at 230–250 K remains on the surface and weakens the adsorption of propylene. We computed the adsorption energy of the system propylene plus H atom at infinite distance (the sum of E_{ads} of the hydrocarbon and of H) and coadsorbed on the same 2×2 unit cell. Our calculations predict a decrease in the adsorption energy of 33 kJ mol^{-1} when both species are coadsorbed, in agreement with the suggestion of Zaera and Chrysostomou [21]. The energy difference arises primarily from the surface-mediated repulsion between reactants sharing bonding with a metal atom [31].

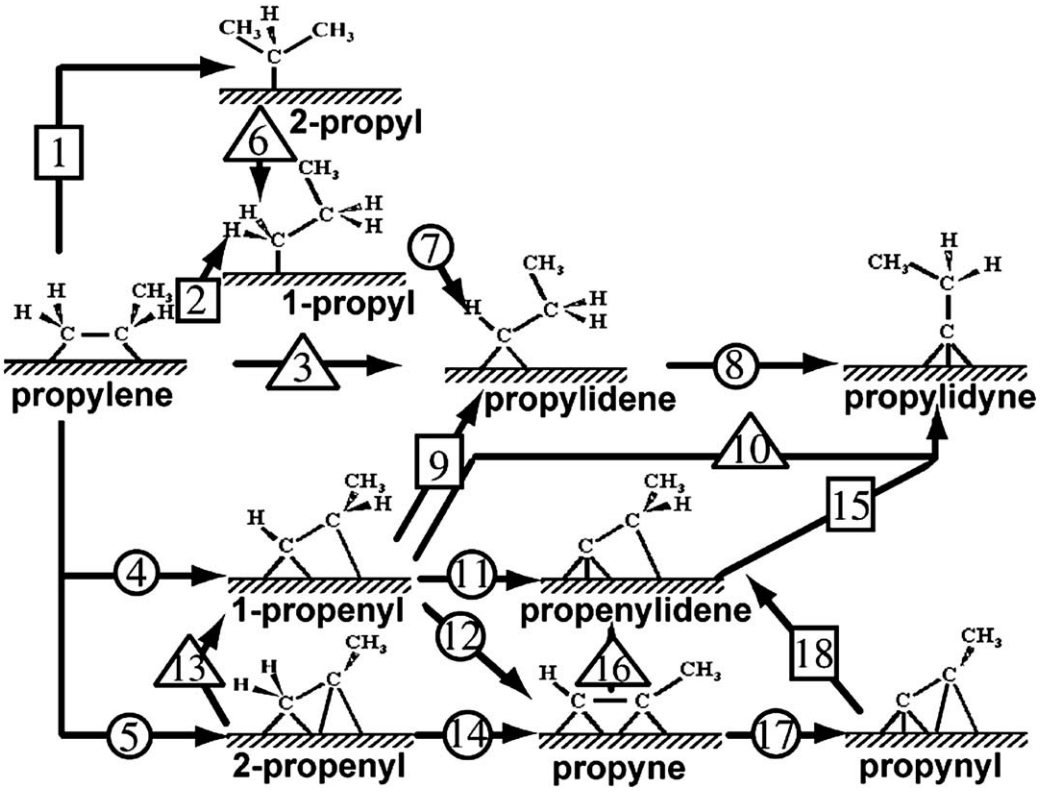

Scheme 2. Elementary paths for the decomposition of propylene to propylidyne on Pt(111). 1, 2, 9, 15 and 18 (□): hydrogenations steps; 4, 5, 7, 8, 11, 12, 14 and 17 (○): dehydrogenation steps and 3, 6, 10, 13 and 16 (△): isomerisation reactions. Numbers from Table 2.

Fig. 1 (side view) summarizes the distortion of propylene and the changes in the Pt–Pt bond distances on adsorption. Gas-phase propylene has a calculated C^1–C^2 bond distance of 1.33 Å and a C^2–C^1H_2 angle (defined as the angle between the C^1–C^2 bond and the C^1H_2 plane) of 180°. On adsorption, the C^1–C^2 distance increases significantly (1.49 Å). Interestingly, this bond distance is close to that obtained for ethylene adsorbed on Pt(111) in a di-σ configuration using a similar computational approach [32,33]. This represents an elongation of 0.15 Å with respect to the gas-phase propylene, thus approaching a single C–C bond length as in propane (1.54 Å) with concomitant reduction of the double-bond character. On adsorption on Pt(111), similar elongations of the C=C bond have also been reported for different alkene molecules [34,35]. Another indicator of the degree of rehybridisation of the C atoms is the C^2–C^1H_2 angle. On Pt(111), propylene loses its "planarity" as the CH bonds bend away from the surface plane. The angle between the H–C^1–H plane and the C^1–C^2 bond (parallel to the surface) is ∼130°.

Scheme 2 displays the elementary paths for the dehydrogenation of di-σ bonded propylene to propylidyne. We did not consider C–C bond cleavage, and we also neglected the dehydrogenation of the methyl group. We determined the adsorption modes and the corresponding adsorption energies for all C_3H_x ($x = 3$–7) species using a 2 × 2 unit cell. The possible reaction intermediates are listed in Table 1. As for propylene [29], we explored different adsorption sites (top, bridge, hollow). Here we show only the most stable identified configuration for each intermediate. The relative stabilities (E_{ads}) for each of the surface species are also shown in Fig. 2.

Table 2
Calculated surface reaction energies (E_{reac}, kJ mol^{-1}) for the decomposition of propylene on Pt(111)

Step	Surface reaction	Reaction	E_{reac}
1	Propylene + H → 2-propyl	Hydrogenation	31
2	Propylene + H → 1-propyl	Hydrogenation	18
3	Propylene → propylidene	Isomerisation	18
4	Propylene → 1-propenyl + H	Dehydrogenation	−6
5	Propylene → 2-propenyl + H	Dehydrogenation	−2
6	2-Propyl → 1-propyl	Isomerisation	−13
7	1-Propyl → propylidene + H	Dehydrogenation	1
8	Propylidene → propylidyne + H	Dehydrogenation	−77
9	1-Propenyl + H → propylidene	Hydrogenation	25
10	1-Propenyl → propylidyne	Isomerisation	−52
11	1-Propenyl → propenylidene + H	Dehydrogenation	−30
12	1-Propenyl → propyne + H	Dehydrogenation	−11
13	2-Propenyl → 1-propenyl	Isomerisation	−4
14	2-Propenyl → propyne + H	Dehydrogenation	−16
15	Propenylidene + H → propylidyne	Hydrogenation	−22
16	Propyne → propenylidene	Isomerisation	−19
17	Propyne → propynyl + H	Dehydrogenation	64
18	Propynyl + H → propenylidene	Hydrogenation	−83

All of the surface intermediates are stable with respect to gas-phase propylene and the clean surface. However, only four moieties are more stable than adsorbed propylene: 1-propenyl, propylidyne, propenylidene, and propyne (see Fig. 2). Among these, the most stable is the propylidyne species. Indeed, propylidyne is 59 kJ mol^{-1} more stable than adsorbed propylene plus

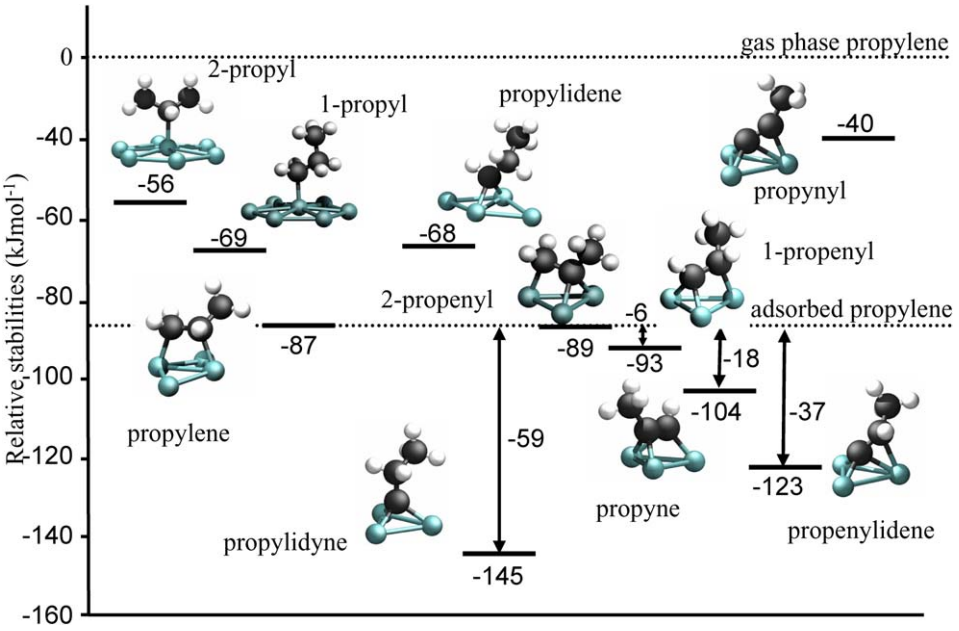

Fig. 2. Energy profile for all the C_3H_x ($x = 3$–7) fragments on Pt(111) at 1/4 ML coverage. Energies in kJ mol^{-1}.

three adsorbed hydrogen atoms. In agreement with the experimental evidence [8,21,23], our calculations confirm that propylene dehydrogenation to propylidyne and surface hydrogen is thermodynamically favourable. Adsorbed 2-propenyl is almost isoenergetic with propylene, with an energy difference of only 2 kJ mol^{-1}. On the other hand, 1-propyl, 2-propyl, propylidene, and propynyl are less stable than adsorbed propylene by 18, 31, 19, and 47 kJ mol^{-1}, respectively.

We investigated the coverage effects for propylene, propylidyne, and two of the possible reaction intermediates (propylidene and 1-propenyl). We increased the size of the unit cell to 3×3 (1/9 ML). In all of the cases, the adsorption energy increased by $\sim$10 kJ mol^{-1}, indicative of a slight repulsion between the hydrocarbon molecules at 1/4 ML coverage (2×2 unit cell). Because the energy difference between the 2×2 and 3×3 systems was roughly the same for all cases, the relative stabilities did not change.

The calculated optimized structural parameters are illustrated in Figs. 3a–3i. For the sake of clarity, only the Pt atoms directly below the hydrocarbon fragment are shown. The 1-propyl (Fig. 3a) and 2-propyl (Fig. 3b) prefer the top adsorption site where the surface metal atom essentially replaces the missing hydrogen atom to form a "propane-like" surface intermediate that preserves its sp^3 symmetry. This is consistent with concepts derived from the orbital integration scheme of Hoffmann [36] and Shustorovich and Baetzold [37]. The balance between the Pauli repulsion and the orbital overlap dictates the adsorption site preference. For metals in the rightmost part of the periodic table, Pauli repulsion dominates [38] and favours the top adsorption site. Neurock and van Santen [39] have rationalized the adsorption site preference of ethyl groups on Pd(111) using these arguments. With respect to propylene, propylidene (Fig. 3c) has two missing hydrogen atoms in C^1 and thus is better adsorbed at a bridge site or η^2(C^1)-adsorption mode. (Here η^2 denotes the number of Pt atoms bind to a C atom.) The C_3H_5

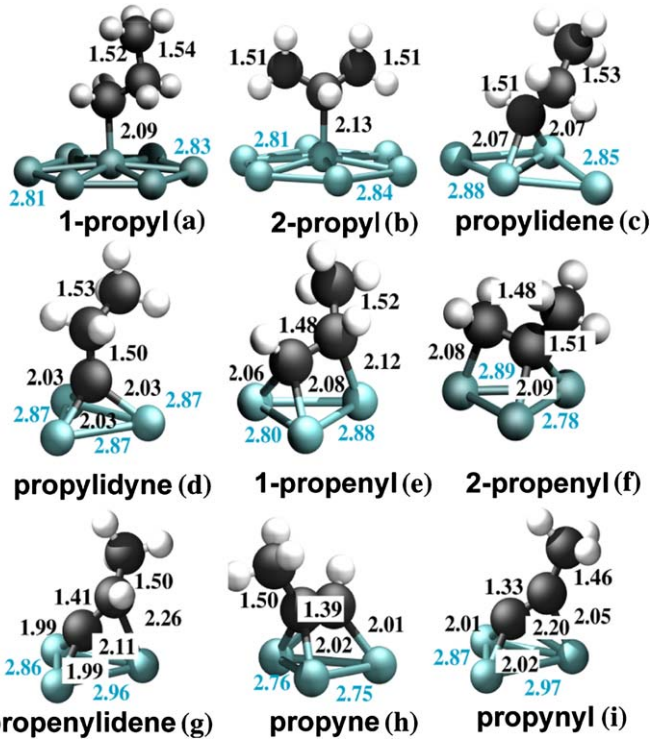

Fig. 3. Adsorption geometries for the C_3H_x ($x = 3$–7) fragments on Pt(111) at 1/4 ML coverage: (a) 1-propyl, (b) 2-propyl, (c) propylidene, (d) propylidyne, (e) 1-propenyl, (f) 2-propenyl, (g) propenylidene, (h) propyne and (i) propynyl. Distances in Å. Only the atoms directly below the hydrocarbon moiety are shown here for sake of visual clarity.

intermediates adsorb preferentially on hollow fcc sites. Propylidyne (Fig. 3d), with three missing hydrogen atoms in C^1, preferentially binds to three Pt atoms in an η^3(C^1) coordination. Our results are in good agreement with the experimental results of Koestner et al. [8]. The 1-propenyl moiety (Fig. 3e) is missing two H atoms in C^1 and one H atom in C^2, and thus it prefers the

$\eta^2\eta^1(C^1,C^2)$-adsorption mode. The adsorption geometry of 2-propenyl (Fig. 3f) is equivalent to that obtained for 1-propenyl. There appears to be a general trend of Pt(111) preferring sp^3-bound intermediates of adsorbed hydrocarbons. Actually, all of the C–C bond distances are within the range of 1.48–1.54 Å.

The pictures for propenylidene (Fig. 3g), propyne (Fig. 3h), and propynyl (Fig. 3i) are quite different. Similar to the C_3H_5 species, these surface intermediates adsorb preferentially on threefold hollow sites (fcc). Three H atoms from C^1 and one atom from C^2 are missing in the propenylidene moiety, and thus this moiety prefers to sit on $\eta^3\eta^1(C^1,C^2)$ coordination. However, the C^1–C^2 bond distance (1.41 Å) is rather short compared with the C_3H_x ($x = 5$–7) hydrocarbon fragments (see above). Dumesic et al. obtained the same adsorption site and geometry for vinylidene ($CH_2{=}C^{\cdot}$) on Pt(111) [40]. Propyne [41] adsorbs on Pt(111) in a $\eta^2\eta^2(C^1,C^2)$ adsorption mode, with the C^1–C^2 (1.39 Å) bond almost parallel to the metal surface. However, propynyl binds in clearly a sp^2 fashion. In this molecule, three H atoms from C^1 and two H atoms from C^2 are missing, which favours the formation of a surface intermediate of sp^3 symmetry; however, it binds to the Pt(111) surface in a $\eta^3\eta^1(C^1,C^2)$ adsorption mode, with the C^2 forming a bond only with a metal atom. Moreover, the C^1–C^2 distance (1.31 Å) is obviously closer to a double bond than to a simple bond. Our results are well in line with those of Jacob and Goddard [42], who investigated the adsorption of the C_2H_y ($y = 1$–5) intermediates on Pt(111) by means of DFT and found that the structure of C_2H_y molecules achieves a saturated configuration in which each C atom is almost tetrahedral. The only exceptions are $CCH^{\cdot}$ (ethynyl) and CHCH (acetylene). Moreover, these authors determined that the alkylidyne moiety is the most strongly bound C_2H_y species.

Table 2 summarizes the reaction energies for the various elementary steps depicted in Scheme 2. We computed the reaction energy (E_{reac}) by subtracting the initial energies from the energies of the final state. For example, we calculated the energy for the propylene dehydrogenation to propylidyne by subtracting the energy of the adsorbed propylene from the energy of the adsorbed propylidyne plus adsorbed H with no interaction between them. We assumed low hydrogen coverage and also that the H atoms attached/released in the hydrogenation/dehydrogenation reactions come from/go to far surface sites.

Most of the elementary steps listed in Table 2 are either slightly endothermic or exothermic and thus will still play a role in propylene decomposition. The most exothermic steps correspond to formation of the propylidyne intermediate. This reaction can occur via hydrogenation, dehydrogenation, or isomerisation. The most favourable way of obtaining this species is from propylidene (-77 kJ mol^{-1}). Moreover, the reaction energies suggest that formation of propynyl is unlikely at this coverage. The formation of this species by dehydrogenation of propyne is uphill by 64 kJ mol^{-1}. Moreover, its hydrogenation to propenylidene is highly exothermic (-84 kJ mol^{-1}). Therefore, we suggest that propynyl is unlikely to be involved in the direct decomposition of propylene to propylidyne. Among all of the possible mechanisms, the two-step reaction pathways ($3 + 8$, propylene → propylidene → propylidyne) and ($4 + 10$, propylene → 1-propenyl → propylidyne) are quite favourable.

Table 3
Experimental frequencies (ν_i, in cm^{-1}) and band assignments, calculated frequencies (ω_i) and intensities (I_i, in kmmol^{-1}) for propylene on Pt(111)

Experimental assignment	RAIRS[a] ν_i	2×2[b] ω_i	I_i	Present assignment
CH_2_as_st	2915(s)	3013	2.2	CH_3_as_st
CH_st	2883(s)	2986	0.1	CH_st
CH_3_s_st + $2CH_3$_as_df	2860(m)	2933	9.9	CH_3_s_st
CH_2_s_st	2830(w)	2982	2.0	CH_2_s_st
–	–	1434/1421	0.4/0.2	CH_3_as_df
CH_2_sci	1437(m)	1400	0.1	CH_2_sci
CH_3_s_df	1375(w)	1337	0.1	CH_3_s_df
CH_b	1309(w)	1296	0.3	CH_b
CH_2_wag	1260(w)	1161	0.2	CH_2_twi
C^2–C^3_st	1088(s)	1092	0.9	C^1–C^2_st/ C^2–C^3_st
CH_2_twi	1037(s)	1030	1.4	CH_2_wag
CH_3_ro	1015(s)	1007	2.9	CH_3_ro

Note. Keys for group frequencies are as: asymmetric; s: symmetric; st: stretching; df: deformation; sci: scissoring; twi: twisting; wag: wagging; ro: rocking; b: bending Keys for intensities are s: strong; m: medium; w: weak.
[a] Values from Ref. [21].
[b] This work.

Table 4
Experimental frequencies (ν_i, in cm^{-1}) and band assignments, calculated frequencies (ω_i) and intensities (I_i, in kmmol^{-1}) for propylidyne on Pt(111)

Experimental assignment	RAIRS[a] ν_i	EELS[b] ν_i	RAIRS[c] ν_i	2×2[d] ω_i	I_i	Theoretical assignment
CH_3_as_st	2960(s)	2980(m)	2961(vs)	3044	5.2	CH_3_as_st
CH_3_s_st	2917(s)	2920(m)	2921(w)/ 2865(mw)	2970	4.4	CH_3_s_st
$2CH_3$_as_df	2860(m)	–	–	–	–	–
CH_3_as_df	1450(m)	1465(s)	1450(s)	1454	1.0	CH_3_as_df
CH_2_sci	1408(m)	–	1407(m)	1399	0.4	CH_2_sci
CH_3_s_df	1374(w)	–	–	1349	0.0	CH_3_s_df
CH_2_wag	–	1295(w)	1303(w)	1265	0.1	CH_2_wag
C–C_st	1104(m)	1115(s)	1103(s)	1087	4.1	C^1–C^2_st
CH_3_ro	1079(w)	1055(s)	1055(w)	1033	0.2	CH_3_ro
CH_3_ro	1041(m)	–	1039(s)	1026	0.0	CH_3_twi
C–C_st	–	920(s)	929(s)	921	1.4	C^2–C^3_st

Note. Keys for group frequencies are as: asymmetric; s: symmetric; st: stretching; df: deformation; sci: scissoring; twi: twisting; wag: wagging; ro: rocking; b: bending Keys for intensities are vs: very strong; s: strong; m: medium; w: weak.
[a] From Ref. [21].
[b] From Ref. [17].
[c] From Ref. [43].
[d] This work.

3.2. Analysis of vibrational spectra

To shed some more light on the nature of the surface intermediate of the propylene dehydrogenation to propylidyne, we computed the RAIRS spectrum for propylene (Table 3), propylidyne (Table 4), and all of the possible reaction intermediates (1-propyl, 2-propyl, propylidene, 1-propenyl, 2-propenyl, propenylidene, propyne, and propynyl; Fig. 4) on Pt(111) at 1/4 ML coverage. Table 3 gives the frequencies along with the

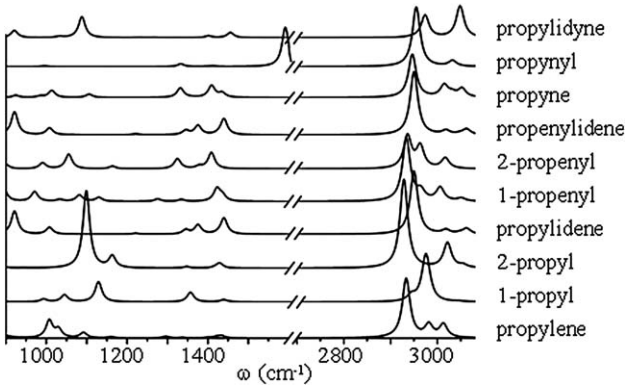

Fig. 4. Simulated RAIRS spectra for propylene, propylidyne and the C_3H_x ($x = 3$–7) intermediates on Pt(111). Intensities in arbitrary units.

intensities for the di-σ propylene on Pt(111). Almost all of the normal modes are coupled. This makes the description of the vibrations somewhat arduous; in some cases, the assignment may be ambiguous. However, our aim is not to analyze in detail the normal modes, but rather to establish the differences among the surface species spectra that can help identify the possible reaction intermediates. Thus, the theoretical assignment accounts for the main vibrations for each feature. The experimental spectrum [21] presents four bands in the C–H stretching region (two of them quite intense), four medium or weak peaks in the 1500–1200 cm^{-1} region, and three intense features in the 1000–1100 cm^{-1} region. Despite some differences in intensities and band assignment, our results are quite consistent with the experimental observations. The differences in the 2800–3100 cm^{-1} region arise from the poor description of the C–H stretching modes, because these modes are strongly affected by anharmonicity. Moreover, both the experimental coverage and the experimental periodicity are not fully reproduced by the present models. The arrangement of the molecules on the surface changes the orientation of the methyl groups and its environment. Zaera and Chrysostomou [21] have pointed out that these changes strongly influence the band intensities.

Table 4 presents the calculated frequencies and intensities for propylidyne on Pt(111). For the sake of comparison, the table also summarizes the corresponding features in the RAIRS [21,43] and EELS spectra [17] of propylene at ∼300 K and saturation coverage. By analogy with the case of ethylene, these studies have determined that these spectra arise from the propylidyne species. Our results fully confirm the experimental assignment (see Table 4). The agreement between the experimental and simulated spectra is fairly good; the main difference appears in the region around 900–1100 cm^{-1}. We assign the features at 1033, 1026, and 921 cm^{-1} to CH_3_ro, CH_3_twi, and C^2–C^3_st, respectively. (For definitions of the normal modes, see the footnotes of Tables 3 and 4.) Only the peaks at 1033 and 920 cm^{-1} are intense. In the experimental RAIRS spectrum, three intense peaks appear in this region. The bands at 1055 [43] (or 1079 [21]), 1039 [43] (or 1041 [21]), and 920 [43] cm^{-1} have been assigned to CH_3_ro, CH_3_ro, and C–C_st, respectively. These differences may arise from the orientations of the neighbouring methyl groups. In our calculations, all of the methyl groups are oriented in the same direction; however, Koestner et al. [8] suggested that the methyl groups tend to minimize the steric repulsions, and thus the steric effect makes some orientations impossible. Obviously, that reproduced with the 2×2 unit cell is not the most favoured.

The spectroscopic information available for the possible intermediates of the propylene-to-propylidyne transformation is scarce. Zaera and Chrysostomou [21] investigated changes in the RAIRS spectrum of propylene on Pt(111) as a function of the temperature (230–300 K) and found indications of the formation of an intermediate. They found that the spectrum at ∼260 K included a new signal at 2890 cm^{-1} and had no new peaks in the C–H deformation IR region. Actually, in the 1000–1500 cm^{-1} region, all of the bands could be assigned to either propylene or propylidyne. These authors proposed that these features may belong to the 2-propyl or to the propylidene species. We simulated and analysed the RAIRS spectra for all of the proposed surface intermediates (Fig. 4). Unfortunately, the C–H stretching region (2800–3100 cm^{-1}) is not well described with the harmonic model. Moreover, all of the features lie within a small range, and the differences are sufficient to be conclusive. Hence we focused our attention on the deformation region. More specifically, the features not present for either propylene or propylidine can help rule out some intermediate species (Fig. 4). The 1-propyl species has two signals at 1125 and 1350 cm^{-1} that are not visible in either the propylene spectrum or the propylidyne spectrum. These features can be assigned to CH_3_s_df and CH_2_wag, respectively. 2-propyl has a quite strong feature at 1162 cm^{-1} (CH_b mixed with CH_3_ro). The propyne molecule and the 2-propenyl and the propenylidene moieties have some important peaks at around 1350 cm^{-1} associated with CH_3_s_df. The propynyl intermediate has a strong feature at 1599 cm^{-1} that can be assigned to C=C_st. However, the experimental spectrum matches the spectrum from propylidene or 1-propenyl, because these species have no important signals in the 1100–1400 cm^{-1} region. Unfortunately, unequivocally identifying the intermediate is impossible.

4. Conclusions

We investigated the adsorption of propylene on Pt(111) at a surface coverage of 0.25 ML using DFT periodic calculations. Moreover, we examined the adsorption modes and energies for various dehydrogenated species: 1-propyl, 2-propyl, propylidene, propylidyne, 1-propenyl, 2-propenyl, propenylidene, propyne, and propynyl. Propylene adsorbs in a bridge adsorption mode with an adsorption energy of −87 kJ mol^{-1}. We determined the relative stabilities and the most favourable adsorption site for propylidyne and all of the possible reaction intermediates. For the C_3H_x ($x = 3$–7) fragments, there appears to be a general trend of Pt(111) preferentially binding to sp^3 carbon intermediates. The relative stabilities of 1-propyl, 2-propyl, propylidene, propylidyne, 1-propenyl, 2-propenyl, propyne, propenylidene, and propynyl are −69, −56, −68, −145, −93, −89, −104, −123, and −40 kJ mol^{-1}, respec-

tively. Propylidyne is the most stable surface species on Pt(111), well in line with the experimental evidence.

We computed the reaction energies for 18 elementary steps that possibly may be involved in the propylene-to-propylidyne transformation. Our calculations clearly indicate that the dehydrogenation of propylene to propylidyne is thermodynamically favourable. The formation of propynyl is energetically unfavourable, and we conclude that this species may not be involved in the direct reaction of dehydrogenation.

In addition, we simulated the vibrational spectra for propylene, propylidyne, and the possible reaction intermediates. Unfortunately, the experimental data available for the reaction intermediate is not sufficient to enable an unequivocal identification. Our best guesses are propylidene and 1-propenyl. It is noteworthy that these two intermediates are not the thermodynamically most stable.

Acknowledgments

This research was supported by the Spanish DGICYT (grants CTQ2005-08459-CO2-01 and CTQ2005-08459-CO2-02) and in part by the Generalitat de Catalunya (GC) (grants 2005SGR-00697 and 2005SGR-00104). F.I. acknowledges support from Distinció de la Generalitat de Catalunya per a la Promoció de la Recerca Universitària. A.V. is grateful to the GC for a predoctoral fellowship. Part of computer time was provided by the Centre de Supercomputació de Catalunya, CESCA, Centre Europeu de Parallelisme de Barcelona, CEPBA, and CEBPA-IBM-Research Institute, CIRI, through grants from Universitat de Barcelona, Fundació Catalana per a la Recerca, and CIRI.

References

[1] F. Zaera, Chem. Rev. 95 (1995) 2651.
[2] N. Sheppard, C. De la Cruz, Adv. Catal. 41 (1996) 1.
[3] T.V.W. Janssens, F. Zaera, J. Catal. 208 (2002) 345.
[4] F. Zaera, Acc. Chem. Res. 25 (1992) 260.
[5] F. Zaera, Isr. J. Chem. 38 (1998) 293.
[6] P.C. Stair, G.A. Somorjai, Chem. Phys. Lett. 41 (1976) 391.
[7] L.L. Kesmodel, L.H. Dubois, G.A. Somorjai, Chem. Phys. Lett. 56 (1978) 267.
[8] R.J. Koestner, J.C. Frost, P.C. Stair, M.A. van Hove, G.A. Somorjai, Surf. Sci. 116 (1982) 85.
[9] L.L. Kesmodel, L.H. Dubois, G.A. Somorjai, J. Chem. Phys. 70 (1979) 2180.
[10] X.-Y. Zhou, X.-Y. Zhu, J.M. White, Surf. Sci. 193 (1988) 387.
[11] D.B. Kang, A.B. Anderson, Surf. Sci. 155 (1985) 639.
[12] A.B. Anderson, S.J. Choe, J. Phys. Chem. 93 (1989) 6145.
[13] E.A. Carter, B.E. Koel, Surf. Sci. 226 (1990) 339.
[14] D. Godbey, F. Zaera, R. Yeates, G.A. Somorjai, Surf. Sci. 167 (1986) 150.
[15] F. Zaera, J. Am. Chem. Soc. 111 (1989) 4240.
[16] M. Salmerón, G.A. Somorjai, J. Phys. Chem. 86 (1982) 341.
[17] N.R. Avery, N. Sheppard, Proc. R. Soc. London A 405 (1986) 1.
[18] A. Cassuto, M. Mane, G. Tourillon, P. Parent, J. Jupille, Surf. Sci. 287/288 (1993) 460.
[19] A.B. Anderson, D.B. Kang, Y. Kim, J. Am. Chem. Soc. 106 (1984) 6597.
[20] Y.-L. Tsai, C. Xu, B.E. Koel, Surf. Sci. 385 (1997) 37.
[21] F. Zaera, D. Chrysostomou, Surf. Sci. 457 (2000) 71;
F. Zaera, D. Chrysostomou, Surf. Sci. 457 (2000) 89.
[22] H. Steininger, H. Ibach, S. Lewald, Surf. Sci. 117 (1982) 685.
[23] C.E. Anson, N. Sheppard, B.R. Bender, J.R. Norton, J. Am. Chem. Soc. 121 (1999) 529.
[24] J.P. Perdew, Y. Wang, Phys. Rev. B 45 (1992) 13244.
[25] G. Kresse, D. Joubert, Phys. Rev. B 59 (1998) 1758.
[26] G. Kresse, J. Hafner, Phys. Rev. B 47 (1993) 558.
[27] G. Kresse, J. Hafner, Phys. Rev. B 48 (1993) 13115.
[28] G. Kresse, J. Hafner, Phys. Rev. B 49 (1994) 14251.
[29] A. Valcárcel, J.M. Ricart, A. Clotet, A. Markovits, C. Minot, F. Illas, Surf. Sci. 519 (2002) 250.
[30] B. Hammer, L.B. Hansen, J. Nørskov, Phys. Rev. B 59 (1999) 7413.
[31] A. Michaelides, Z.-P. Liu, C.J. Zhang, A. Alavi, D.A. King, P. Hu, J. Am. Chem. Soc. 125 (2003) 3704.
[32] Q. Ge, D.A. King, J. Chem. Phys. 110 (1999) 4699.
[33] G.W. Watson, R.P.K. Wells, D.J. Willock, G.J. Hutchings, J. Phys. Chem. B 104 (2000) 6439.
[34] A. Valcárcel, A. Clotet, J.M. Ricart, F. Delbecq, P. Sautet, Surf. Sci. 549 (2004) 121.
[35] Q. Ge, D.A. King, J. Chem. Phys. 110 (1999) 4699.
[36] R. Hoffmann, Solids and Surfaces, VCH, New York, 1988.
[37] E. Schustorovich, R.C. Baetzold, Science 227 (1985) 876.
[38] R.A. van Santen, Catal. Lett. 16 (1992) 59.
[39] M. Neurock, R.A. van Santen, J. Phys. Chem. B 104 (2000) 11127.
[40] S.G. Podkolzin, R. Alcalà, J.A. Dumesic, J. Mol. Catal. A 218 (2004) 217.
[41] A. Valcárcel, J.M. Ricart, A. Clotet, A. Markovits, C. Minot, F. Illas, J. Chem. Phys. 116 (2002) 1165.
[42] T. Jacob, W.A. Goddard III, J. Phys. Chem. B 109 (2005) 297.
[43] M.A. Chesters, C. de la Cruz, P. Gadner, E.M. McCash, P. Pudney, G. Shahid, N. Sheppard, J. Chem. Soc., Faraday Trans. 86 (1990) 2757.